Vibration control with optimized sliding surface for active suspension systems using geophone

Vibration control with optimized sliding surface for active suspension systems using geophone

Chenyang Ding[1], A.A.H. Damen[1], and P.P.J. van den Bosch[1]

[1]Eindhoven University of Technology, P.O. Box 513, Eindhoven, 5600MB,The Netherlands email: c.ding@tue.nl, a.a.h.damen@tue.nl, p.p.j.v.d.bosch@tue.nl

ABSTRACT

The frequency shaped sliding surface approach has been proposed for control of a suspension system measured by a relative displacement sensor and an absolute velocity sensor (geophone). The vibration isolation performance (transmissibility) is determined by the sliding surface design. The direct disturbance-force rejection performance (compliance) is determined by the regulator design. The sliding surface was designed by the pole placement method in our previous work. But manual pole placement is difficult to achieve the optimal performance. This paper formulates the problem of sliding surface optimization taking into account the geophone dynamics and solves it using Matlab optimization toolbox. The vibration isolation performance designed by sliding surface optimization is much better than the manual pole placement. The regulator is designed to realize the designed performances and to reduce the compliance.

1 INTRODUCTION

The performance of the suspension system is crucial in many high-precision machines. A typical example is the photolithographic wafer scanner used to manufacture the integrated circuits up to nanometer details. In this machine, a six Degrees-Of-Freedom (DOF) suspension system is applied to inertially fix the metrology frame (payload) despite of all disturbances, including the vibrations transmitted from the floor and the directly applied disturbance forces. As the payload is extremely sensitive to any disturbances, mechanical contacts between the payload and the environment are not desired. If all mechanical contacts are eliminated, not only the payload has to be stabilized at all six DOFs, but also the compensation of the payload gravity force (in the order of 10^4 N) with low energy consumption becomes a challenge. The current contactless suspension system applied in the industry is based on pneumatic isolators [1]. The 6-DOF suspension system based on electromagnetic isolators, which compensates the payload gravity by passive permanent magnetic force, is also feasible [2] and being investigated [3] as an alternative. For a multi-DOF system, the decentralized control which combines 1-DOF control and decoupling matrices can be applied to reduce the implementation cost. The decoupling performance is improved by the recent developed algorithm [4]. In this way, 1-DOF vibration control can be applied to multi-DOF systems. For this reason, control of 1-DOF suspension system is studied.

The objective of the vibration control is to minimize the plant absolute displacement (the terminology *absolute* indicates that this physical value is with respect to an inertially fixed reference). The performance of the suspension system is evaluated by two frequency domain criterions. The *transmissibility*, defined by the transfer function from the floor vibration to the payload vibration, is used to evaluate the vibration isolation performance. The *compliance*, defined by the transfer function from the force disturbance to the payload vibration, is used to evaluate the disturbance rejection performance. The compliance has the lower priority because the effect of the disturbances can also be reduced by other means. For example, vacuum operation eliminates the acoustic noises. Nevertheless, the compliance should not be compromised while improving the transmissibility. With only the relative displacement feedback, it is not possible to improve the transmissibility without compromising the compliance. Therefore, the feedback scheme of relative displacement and payload absolute velocity is widely applied in the industry.

Geophone is well-known for its low-cost absolute velocity measurement. However, its dynamic characteristics [5] limit its performance at low frequencies. The measurement gain decays with decreasing frequency lower than its resonant frequency and it is zero for DC velocity. Since the geophone circuitry noise does not decay with frequency, the signal to noise ratio of the geophone reduces rapidly while decreasing the frequency. Therefore, low frequency vibration isolation using geophone is challenging.

The most popular vibration control algorithm is the skyhook control [6] which is the proportional control of the absolute velocity. The skyhook control is able to reduce or even remove the resonance peak but vibration isolation improvement at low frequencies is difficult. The H_∞ control [7] can be directly applied to solve the multi-DOF vibration control design problem. It depends on the weighting filters design to optimize the closed-loop performance. But this design process is complicated and usually requires many iterations to complete. Besides, the H_∞ controller usually has high order which limits its application.

In our previous work [8], the frequency-shaped sliding surface control proposed in [5] is generalized as a two-step vibration control design method. The transmissibility and the sensitivities are determined by the sliding surface design and the compliance is designed by the regulator. The pole placement method can be used to tune the transmissibility and the sensitivity taking the geophone dynamics into account but the tuning process is cumbersome.

This paper formulates a sliding surface optimization problem based on common industrial requirements, floor vibration strength and sensor performances. Subsequently, it is solved numerically using Matlab optimization tool-

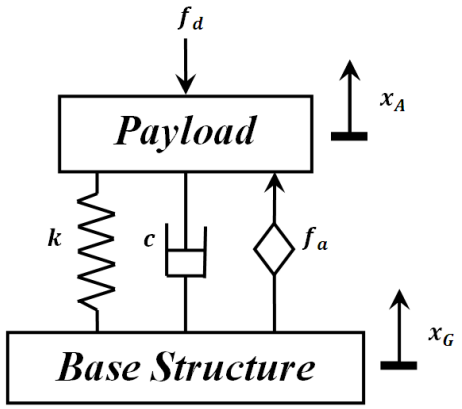

Figure 1: Physical model of the 1-DOF suspension system.

box. The optimization result determines the three designed performances: transmissibility and the two sensitivity functions. Section 2 introduces the model of a 1-DOF suspension system and the installed sensors. Performance requirements are also described. Section 3 reviews the generalized frequency-shaped sliding surface control. Section 4 describes the formulation of the sliding surface optimization problem and gives a numerical example. The conclusion is given in Section 5.

2 Problem Formulation

2.1 1-DOF Model

A 1-DOF model is introduced as an example plant to study the vibration control. The physical model of the 1-DOF plant is shown in Fig. 1. The base structure represents the floor. The payload mass, spring stiffness, and damping coefficient are denoted by m, k, and c, respectively. The payload absolute displacement, payload absolute velocity, and floor absolute displacement are denoted by x_A, v_A, and x_G, respectively. The actuator force and the directly applied disturbance force are denoted by f_a and f_d, respectively. The equation of motion for the payload is given by

$$m\dot{v_A} + c\dot{x_R} + kx_R = f_a - f_d, \tag{1}$$

where $x_R = x_A - x_G$ is the relative displacement. The diagram of the physical model is shown in the dashed rectangular in Fig. 2.

2.2 Sensor Models

The signals used for control are the payload relative displacement x_R and the payload absolute velocity v_A. The signals $\widetilde{x_R}$ and $\widetilde{v_A}$ are the measured x_R and v_A, respectively. The displacement sensor usually has very high bandwidth (in the order of 10^4 Hz) so that the sensor dynamics is negligible at low frequencies (in the order of 10^2 Hz or lower). The displacement sensor noise, denoted by n_x, is assumed to be independent of x_R so that $\widetilde{x_R}$ is derived by

$$\widetilde{x_R} = x_R + n_x. \tag{2}$$

Geophone is a type of absolute velocity sensor widely used in the industry. The dynamic model [5] for the geophone has the form of

$$G_v(s) = \frac{s^2}{s^2 + 2\omega_v\xi_v s + \omega_v^2}, \tag{3}$$

where ω_v is the resonant frequency and ξ_v is the damping ratio. The geophone noise, denoted by n_v, is assumed to be independent of v_A. The relation between $\widetilde{v_A}$ and v_A is

$$\widetilde{v_A} = G_v(s)v_A + n_v. \tag{4}$$

2.3 Performance Requirements

There are four closed-loop performances. Besides the transmissibility $\mathbb{T}_c$ and the compliance $\mathbb{C}_c$, the two sensitivity functions $\mathbb{S}_c$ and $\mathbb{R}_c$ are also concerned. The sensitivity $\mathbb{S}_c$ is the transfer from the geophone sensor noise to payload vibration. The sensitivity $\mathbb{R}_c$ is the transfer from the displacement sensor noise to the payload vibration. $\mathbb{S}_c$ and $\mathbb{R}_c$ are concerned because they would affect $\overline{|\mathbb{T}_c|}$, the upper bound of $|\mathbb{T}_c|$.

The fundamental constraints are

1 $\mathbb{T}_c$, $\mathbb{C}_c$, $\mathbb{S}_c$, and $\mathbb{R}_c$ are all stable.

2 Interested frequency range is up to the order of 10^2 Hz.

3 $|\mathbb{T}_c(0)| = 1$ (0 dB).

4 $\frac{d|\mathbb{T}_c(\omega)|}{d\omega} \leq -40$ dB/dec at high frequencies.

5 $|\mathbb{S}_c(0)| = 0$ ($-\infty$ dB). This item is to filter the acceleration sensor DC bias.

6 $|\mathbb{C}_c(0)| = 0$ ($-\infty$ dB) is preferred.

For all $\mathbb{T}_c$, $\mathbb{C}_c$, $\mathbb{S}_c$, and $\mathbb{R}_c$, lower magnitude indicates better performance. For $\mathbb{T}_c$, lower cross-over frequency indicate better performance. Note that it is impossible to simultaneously improve all performances at a certain frequency. Among all the four performances, $\mathbb{T}_c$ is the most important one. As industrial environments usually have vibrations at a certain frequency, $\overline{|\mathbb{T}_c|}$ is required to be smaller than some desired value at these frequencies while its resonance peak is minimized. Based on these requirements, the optimized transmissibility is defined as follows.

Assume that the cut-off frequency of $\overline{|\mathbb{T}_c|}$, denoted by ω_c, has a required upper-bound, ω_1. Assume that ω_i and ε_i, $\forall\, i \in \{0,1,2,...,n\}$ are predefined constants that satisfy

- $\omega_0 < \omega_c$.
- $\omega_1 = \omega_c$.
- $\omega_i > \omega_c \;\forall\, i \in \{2,3,...,n\}$.
- $\varepsilon_0 > 1$.
- $\varepsilon_1 = 1$.
- $\varepsilon_i < 1 \;\forall\, i \in \{2,3,...,n\}$.

Let a denote a set of controller parameters to be designed. The sliding surface optimization is to find a set $\hat{a}$ which minimizes the resonance peak of the transmissibility upper bound under constraints.

$$\hat{a} = \min_{a} \sup_{\omega} \overline{|\mathbb{T}_c(\omega)|}, \tag{5}$$

under the constraints of

- $\overline{|\mathbb{T}_c(\omega)|} \leq \varepsilon_0, \forall\, \omega \leq \omega_0$.
- $\overline{|\mathbb{T}_c(\omega_i)|} \leq \varepsilon_i, \forall\, i \in \{1,2,...,n\}$.

Note that the above constraints are the most common industrial requirements for a suspension system.

3 Generalized Sliding Surface Control

The frequency-shaped sliding surface control (or sliding surface control for short) is physically interpreted to vibration control by L. Zuo and J.J.E. Slotine [5] in 2004. Therein, the sliding surface is designed for ideal feedback signals. It is generalized as a two-step vibration control design method in our previous work [8]. This section provides a brief review.

The control of the 1-DOF system using sliding surface control is illustrated in the diagram in Fig. 2. The sliding surface is defined by the equation $\sigma = 0$. The blocks Λ_1 and Λ_2 are two transfer functions used to shape the sliding surface. The block R is the regulator. The generalized sliding surface control is a two-step control design method. The first step is to design the sliding surface (Λ_1 and Λ_2) which determines the designed performances. The second step is to design the regulator R to guarantee the convergence of σ to zero. As long as this convergence is guaranteed, the designed performances can be realized.

3.1 Sliding Surface Equation

The designed performances, which are determined by Λ_1 and Λ_2, are the designed transmissibility $\mathbb{T}_d$ and the two designed sensitivity functions $\mathbb{R}_d$ and $\mathbb{S}_d$. They are defined as

$$\mathbb{T}_d = -\mathbb{R}_d = \frac{\Lambda_1}{\Lambda_1 + \Lambda_2 s G_v}, \mathbb{S}_d = \frac{-\Lambda_2}{\Lambda_1 + \Lambda_2 s G_v}. \tag{6}$$

According to Fig. 2, the equation $\sigma = 0$ is equivalent to

$$\Lambda_1 \widetilde{x_R} + \Lambda_2 \widetilde{v_A} = 0. \tag{7}$$

Substitute (2) and (4) into (7), we have

$$\Lambda_1 (x_R + n_x) + \Lambda_2 (G_v v_A + n_v) = 0. \tag{8}$$

By applying the Laplace Transform, it can be subsequently used to calculate $\overline{|\mathbb{T}_d|}$, the upper bound of the designed transmissibility magnitude.

$$\frac{X_A}{X_G} = \frac{\Lambda_1}{\Lambda_1 + \Lambda_2 s G_v}\left(1 - \frac{N_x}{X_G}\right) - \frac{\Lambda_2}{\Lambda_1 + \Lambda_2 s G_v}\frac{N_v}{X_G}, \tag{9}$$

where X_A, X_G, N_x, and N_v are Laplace Transform of signals x_A, x_G, n_x, and n_v, respectively. According to (9), $\overline{|\mathbb{T}_d|}$ can be derived as

$$|\mathbb{T}_d| \leqslant \overline{|\mathbb{T}_d|} = |\mathbb{T}_d| + |\mathbb{R}_d|\left|\frac{N_x}{X_G}\right| + |\mathbb{S}_d|\left|\frac{N_v}{X_G}\right|. \tag{10}$$

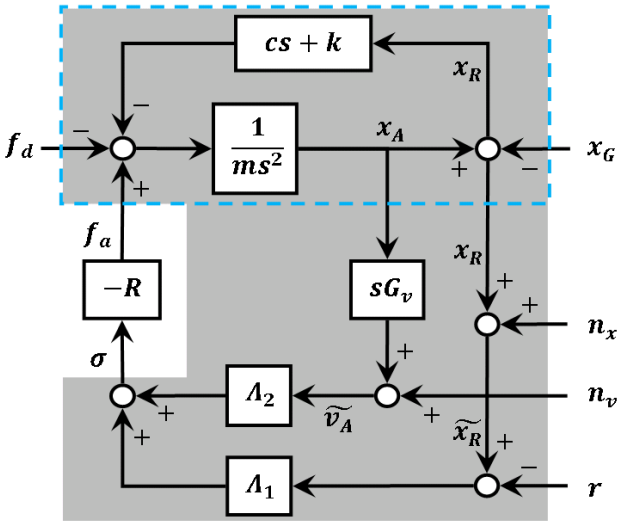

Figure 2: Generalized FSSSC diagram.

To make $\mathbb{T}_d$ more robust against the sensor noise, its upper bound has to be reduced. Among all the possible ways to achieve that, reducing $|\mathbb{S}_d|$ is the only way in the field of control design, which relies on the sliding surface design. According to (6), $\mathbb{S}_d$ and $\mathbb{T}_d$ are related by

$$\mathbb{T}_d + s G_v \mathbb{S}_d = 1. \tag{11}$$

Therefore, to simultaneously improve both $\mathbb{S}_d$ and $\mathbb{T}_d$ is impossible with predefined geophone dynamics. The sliding surface design has to make a trade-off between $\mathbb{S}_d$ and $\mathbb{T}_d$.

3.2 Regulator Design

The objective of the regulator design is to realize the designed performances by keeping $\sigma = 0$. The vibration isolation of the original plant is therefore transformed to the regulation of a new system P_n which is composed of the original plant and the designed sliding surface (Λ_1 and Λ_2). The input is the control force f_a and the output is σ (note that σ is exactly known). The transfer function of P_n is derived according to the shaded blocks in Fig. 2.

$$P_n = (\Lambda_1 + \Lambda_2 s G_v)\frac{1}{ms^2 + cs + k}. \tag{12}$$

The regulator R has to be designed according to the properties of P_n to keep σ zero. If the plant P_n is linear, the regulation can be as simple as PID even if $\mathbb{C}_c(0) = 0$ is required. More advanced methods like optimal control or H_∞ control can also apply. If there exist significant nonlinearity in P_n (due to the original plant), there are also many candidate design methods, for example, back-stepping, sliding mode control, etc.

In [5], the conventional switching control is directly applied as the regulator to reject the unknown disturbances and an adaptive algorithm is proposed to deal with the plant parameter uncertainties. The switching control is described as

$$f_a = -f \cdot \mathrm{sgn}(\sigma), \tag{13}$$

where f is a positive constant. Since the sliding surface is much more complicated than that in [5], directly applied switching control might not be able to stabilize P_n. If that is the case, the conventional sliding mode control can be applied to guarantee the convergence of σ to zero under all the unknown disturbances. Boundary layer control can be designed to reduce the chatter. However, boundary layer control rely on linear control design tools [9]. In either cases, switching control or sliding mode control, $\mathbb{T}_d$ and $\mathbb{S}_d$ can be approximately realized.

If the regulator is linear, the FSSSC approach is a linear approach. Based on the linear plant (if it is nonlinear, we assume it can be linearized around a working point), the closed-loop transmissibility $\mathbb{T}_c$ and compliance $\mathbb{C}_c$ can be calculated based on Fig. 2.

$$\mathbb{T}_c = \frac{\Lambda_1 + \frac{cs+k}{R}}{\frac{1}{PR} + \frac{cs+k}{R} + \Lambda_1 + \Lambda_2 s G_v}, \tag{14}$$

$$\mathbb{C}_c = \frac{\frac{1}{R}}{\frac{1}{PR} + \frac{cs+k}{R} + \Lambda_1 + \Lambda_2 s G_v}, \tag{15}$$

where $P = \frac{1}{ms^2}$. The closed-loop geophone-noise sensitivity $\mathbb{S}_c$ is calculated as

$$\mathbb{S}_c = \frac{-\Lambda_2}{\frac{1}{PR} + \frac{cs+k}{R} + \Lambda_1 + \Lambda_2 s G_v}. \tag{16}$$

The closed-loop displacement-sensor-noise sensitivity $\mathbb{R}_c$ is calculated as

$$\mathbb{R}_c = \frac{-\Lambda_1}{\frac{1}{PR} + \frac{cs+k}{R} + \Lambda_1 + \Lambda_2 s G_v}. \tag{17}$$

The upper bound of the closed-loop transmissibility magnitude, $|\overline{\mathbb{T}_c}|$, is calculated as

$$|\mathbb{T}_c| \leqslant |\overline{\mathbb{T}_c}| = |\mathbb{T}_c| + |\mathbb{R}_c| \left| \frac{N_x}{X_G} \right| + |\mathbb{S}_c| \left| \frac{N_v}{X_G} \right|. \tag{18}$$

If the open loop gain is so high that the approximations

$$\Lambda_1 + \frac{cs+k}{R} \approx \Lambda_1, \tag{19a}$$

$$\frac{1}{PR} + \frac{cs+k}{R} + \Lambda_1 + \Lambda_2 s G_v \approx \Lambda_1 + \Lambda_2 s G_v, \tag{19b}$$

are feasible, we have $\mathbb{T}_c = \mathbb{T}_d$, $\mathbb{R}_c = \mathbb{R}_d$ and $\mathbb{S}_c = \mathbb{S}_d$. Also, the upper bound in (18) is exactly the same as (10) and $|\mathbb{C}_c|$ is reduced. Therefore, R has to be designed as a high-gain controller to make the approximation (19) feasible. As a result, design of $\mathbb{T}_c$ and $\mathbb{S}_c$ can be accomplished by the sliding surface design. The bottle neck to increase the open-loop gain would be the actuator capacity, the control-loop time-delay, and unmodeled flexible modes.

4 Sliding Surface Design

4.1 Manual Pole Placement

Our previous work [8] transforms the sliding surface design problem into a manual pole placement problem. Denote the numerators and denominators of $\Lambda_i, \forall i \in \{1,2\}$ by N_i and D_i, respectively, (6) becomes

$$\mathbb{T}_d = \frac{N_1 D_2 (s^2 + 2\omega_v \xi_v s + \omega_v^2)}{N_1 D_2 (s^2 + 2\omega_v \xi_v s + \omega_v^2) + N_2 D_1 s^3}, \tag{20a}$$

$$\mathbb{S}_d = -\frac{N_2 D_1 (s^2 + 2\omega_v \xi_v s + \omega_v^2)}{N_1 D_2 (s^2 + 2\omega_v \xi_v s + \omega_v^2) + N_2 D_1 s^3}. \tag{20b}$$

Let $D_1 = (s^2 + 2\omega_v \xi_v s + \omega_v^2) D_2$, (20) is simplified to

$$\mathbb{T}_d = \frac{N_1}{N_1 + N_2 s^3}, \qquad \mathbb{S}_d = -\frac{N_2 (s^2 + 2\omega_v \xi_v s + \omega_v^2)}{N_1 + N_2 s^3}. \tag{21}$$

To achieve $\mathbb{S}_d(0) = 0$, the constant term of the polynomial N_2 should be zero. Let $N_2 = N_2' s$, (21) becomes

$$\mathbb{T}_d = \frac{N_1}{N_1 + N_2' s^4}, \qquad \mathbb{S}_d = -\frac{N_2' s (s^2 + 2\omega_v \xi_v s + \omega_v^2)}{N_1 + N_2' s^4}. \tag{22}$$

$\mathbb{T}_d$ can be designed by the choice of N_1 and N_2'. To achieve the -40 dB/dec decreasing rate of $|\mathbb{T}_d|$ at high frequencies, the denominator order should be the numerator order plus two. If the order of $\mathbb{T}_d$ is *four* (this is the lowest), N_2' has to be a constant and the order of N_1 has three possibilities: zero, one or two. In this case, $\mathbb{T}_d$ has the possible forms of

$$\mathbb{T}_d = \frac{a_0}{a_4 s^4 + a_0},$$
$$\text{or } \mathbb{T}_d = \frac{a_1 s + a_0}{a_4 s^4 + a_1 s + a_0},$$
$$\text{or } \mathbb{T}_d = \frac{a_2 s^2 + a_1 s + a_0}{a_4 s^4 + a_2 s^2 + a_1 s + a_0}.$$

To make $\mathbb{T}_d$ stable, proper sets of constants $\{a_0, a_4\}$ or $\{a_0, a_1, a_4\}$ or $\{a_0, a_1, a_2, a_4\}$ have to be found, which are difficult.

If the order of $\mathbb{T}_d$ is *five*, the two numerators can be designed as $N_1 = a_3 s^3 + a_2 s^2 + a_1 s + a_0$ and $N_2' = a_5 s + a_4$ so that $\mathbb{T}_d$ has the form of

$$\mathbb{T}_d = \frac{a_3 s^3 + a_2 s^2 + a_1 s + a_0}{a_5 s^5 + a_4 s^4 + a_3 s^3 + a_2 s^2 + a_1 s + a_0}. \tag{23}$$

And $\mathbb{S}_d$ has the form of

$$\mathbb{S}_d = -\frac{(a_5 s^2 + a_4 s)(s^2 + 2\omega_v \xi_v s + \omega_v^2)}{a_5 s^5 + a_4 s^4 + a_3 s^3 + a_2 s^2 + a_1 s + a_0}. \tag{24}$$

The five poles of $\mathbb{T}_d$ can be selected based on criterions of stability and low resonant frequency. Subsequently, the constants $a_i, \forall i \in \{0,1,2,3,4,5\}$ are determined. In this design, both $\mathbb{T}_d$ and $\mathbb{S}_d$ fulfill the design criterions. The design of D_1 and D_2 is to make Λ_1 and Λ_2 stable and to simplify the regulator design. If we continue increasing the order of $\mathbb{T}_d$, higher decreasing rate of $|\mathbb{T}_d|$ or lower $|\mathbb{S}_d|$ can be achieved. The price would be the increased order of the controller.

The pole placement in the sliding surface design can be accomplished manually but it would be a cumbersome process. A optimization process using Matlab optimization toolbox could be a good alternative.

4.2 Preparation for Optimization

The frequency response of a geophone is usually plotted in the sensor specification documents. The parameters of G_v can be estimated. The Power Spectrum Density (PSD) of the sensor noises (n_x and n_a) can be experimentally measured [10]. Similarly, the PSD of the base acceleration can also be experimentally measured. The PSD ratios of the sensor noises over the base-frame displacement vary with the frequency. These variations can be described by two functions.

$$G_x(\omega) = \frac{N_x(\omega)}{X_G(\omega)},\ G_v(\omega) = \frac{N_v(\omega)}{X_G(\omega)}. \tag{25}$$

Note that both $G_x(\omega)$ and $G_v(\omega)$ can be either continuous functions or look-up tables. (10) can be reformed to

$$\overline{|\mathbb{T}_d(\omega)|} = |\mathbb{T}_d(\omega)|(1+|G_x(\omega)|) + |\mathbb{S}_d(\omega)||G_v(\omega)|. \tag{26}$$

There are two ways to parameterize the cost function $\overline{|\mathbb{T}_d(\omega)|}$. They are described as follows.

4.3 Poles Parameterization

Assume that $\mathbb{T}_d$ takes the form of (23), there are four possibilities of the five poles. Assume that $r_i < 0, \forall\, i \in \{1,2,3,4,5\}$ are independent negative variables, the three possible combinations of the five stable poles are

- Five real poles ($r_i,\ \forall\, i \in \{1,2,3,4,5\}$).
- Three real poles ($r_i,\ \forall\, i \in \{1,2,3\}$) and a conjugate pair ($r_4 \pm r_5 j$).
- One real pole (r_1) and two conjugate pairs ($r_2 \pm r_3 j$ and $r_4 \pm r_5 j$).

In each case, $\overline{|\mathbb{T}_d(\omega)|}$ can be numerically calculated according to (26) and (23). The sliding surface optimization is formulated as follows.

To find the set of four negative variables $r_i, \forall\, i \in \{1,2,3,4,5\}$ which minimizes $\sup \overline{|\mathbb{T}_d(\omega)|}$ under constraints of

- $\overline{|\mathbb{T}_d(\omega)|} \le \varepsilon_0, \forall\, \omega \le \omega_0$.
- $\overline{|\mathbb{T}_d(\omega_i)|} \le \varepsilon_i, \forall\, i \in \{1,2,...,n\}$.

The above optimization problem can be solved numerically in Matlab for each case of pole combinations. The final optimal solution is the one with lowest $\sup \overline{|\mathbb{T}_d(\omega)|}$.

4.4 Denominator Parameterization

Assume that $\mathbb{T}_d$ takes the form of (23), the constants $a_i,\ \forall\, i \in \{0,1,2,3,4\}$ are used as parameters and the constant a_5 is set to one without losing generality. The sliding surface optimization is formulated as follows.

To find the set of four positive variables $a_i, \forall\, i \in \{0,1,2,3,4\}$ which minimizes $\sup \overline{|\mathbb{T}_d(\omega)|}$ under constraints of

- $\overline{|\mathbb{T}_d(\omega)|} \le \varepsilon_0, \forall\, \omega \le \omega_0$.
- $\overline{|\mathbb{T}_d(\omega_i)|} \le \varepsilon_i, \forall\, i \in \{1,2,...,n\}$.
- $a_i > 0, \forall\, i \in \{0,1,2,3,4\}$.
- $b_1 = a_3 - a_2/a_4 > 0$.
- $c_1 = a_2 - b_2 a_4/b_1 > 0$, where $b_2 = a_1 - a_0/a_4$.
- $b_2 - b_1 a_0/c_1 > 0$, where $b_2 = a_1 - a_0/a_4$.

The last four constraints are used to keep $\mathbb{T}_d$ stable. They are derived using the Routh-Hurwitz criterion.

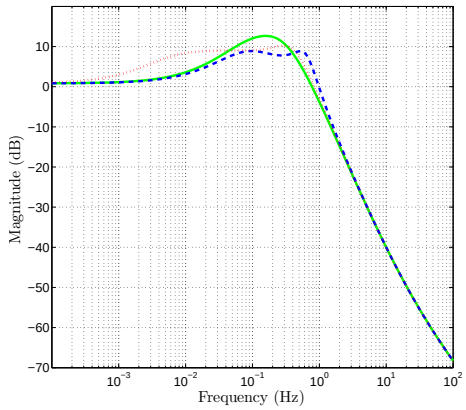

Figure 3: Corresponding optimized $\overline{|\mathbb{T}_d|}$ using the pole parameterization. The solid line (blue) is the result of four real pole parameterization. The dashed line (red) is the result of two real poles & a conjugate pair parameterization.

4.5 Numerical Example

A simple numerical example of the optimization process is given. Assume that

- $\omega_v = 2\pi$ rad/s and $\xi_v = 0.7$.
- $|G_x(\omega)| = 0.1$ and $|G_v(\omega)| = 0.2$.
- $\omega_0 = 0.001$ Hz, $\omega_1 = 1$ Hz, $\omega_2 = 10$ Hz.
- $\varepsilon_0 = 1.4125$ (3 dB), $\varepsilon_1 = 1$ (0 dB), $\varepsilon_2 = 0.01$ (-40 dB).

Using the pole parameterization, the initial values are set as $r_i = -1,\ \forall\, i \in \{1,2,3,4,5\}$. Three results are obtained for each combination of the four poles.

- Five real poles ($r_i = -1.5632,\ \forall\, i \in \{1,2,3,4,5\}$).
- Three real poles ($r_1 = -0.7670$, $r_2 = -0.8573$, $r_3 = -0.7327$) and a conjugate pair ($-1.4248 \pm 3.7058 j$).
- One real and Two conjugate pairs (-0.0345, $-1.7862 \pm 1.5838 j$ and $-1.7861 \pm 1.5836 j$).

Since the results of four real poles and two conjugate pairs converge, there are only two different results left. The corresponding $\overline{|\mathbb{T}_d|}$ curves are plotted in Fig. 3. The second pole combination (two real poles and one conjugate pair) gives the lowest peak of $\overline{|\mathbb{T}_d|}$ (8.8806 dB) so that it is the optimized solution.

Using the denominator parameterization, the initial values are set as $a_4 = 5$,$a_3 = 10$, $a_2 = 10$, $a_1 = 5$, and

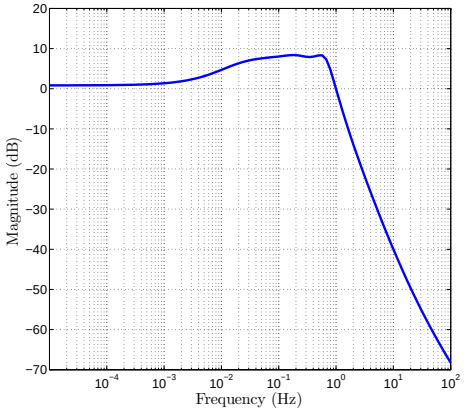

Figure 4: Corresponding optimized $\overline{|\mathbb{T}_d|}$ using the denominator parameterization.

$a_0 = 1$. Note that this set of initial values places five real poles at -1. But the result is not as good as that of pole parameterization. Therefore, the results of pole parameterization are used as initial values. The optimized parameters are $a_4 = 4.7503$, $a_3 = 24.3178$, $a_2 = 35.3461$, $a_1 = 31.5798$, and $a_0 = 3.4184$. The corresponding $\overline{|\mathbb{T}_d|}$ curve is plotted in Fig. 4. The peak value is 8.3794 dB, which is lower than the pole parameterization method.

4.6 Remarks

Note that the optimization process in Matlab does not guarantee the existence of the solution. Therefore, the initial values of the optimization process should satisfy all the constraints. The two parameterization methods give different results. This is because the optimization process in Matlab does not guarantee global optimum. One way to further improve the optimization performance is to iteratively run the optimization process using the result of the previous optimization process as the initial values. But the improvement gained by using this iteration is usually ignorably small in practice. Nevertheless, the optimization process is more straightforward. To derive a sliding surface that is comparable to the optimized sliding surface using the manual pole placement would be a cumbersome process.

5 CONCLUSION

This paper reviews the application of the frequency-shaped sliding surface to vibration control design. A sliding surface optimization problem is formulated based on the floor vibration strength, performance requirements, and the sensor noise conditions. The numerical example shows that the sliding surface design using the optimization toolbox in Matlab is feasible. The sliding surface design using the proposed optimization process is more straightforward the manual pole placement. Although Matlab does not guarantee global optimum, to derive a sliding surface that is comparable to the optimized sliding surface using the manual pole placement would be a cumbersome process.

This paper focuses on 1-DOF suspension system control design. Incorporating static decoupling matrices derived by static optimal decoupling [4] or modal decomposition [11], this approach is also applicable to multi-DOF suspension systems.

6 ACKNOWLEDGMENTS

This work is a part of the Dutch IOP-EMVT program and is supported financially by SenterNovem, an agency of the Dutch Ministry of Economic Affairs.

REFERENCES

[1] M. Heertjes and N. van de Wouw, "Nonlinear dynamics and control of a pneumatic vibration isolator," *ASME Journal of Vibration and Acoustics*, vol. 128, pp. 439–448, 2006.

[2] J. Janssen, J. Paulides, and E. Lomonova, "Passive limitations for a magnetic gravity compensator," *Journal of System Design and Dynamics*, vol. 3, no. 4, pp. 671–680, 2009.

[3] C. Ding, J. Janssen, A. Damen, and P. v. d. Bosch, "Modeling and control of a 6-dof contactless electromagnetic suspension system with passive gravity compensation," in *Proc. of XIX International Conference on Electrical Machines*, (Roma, Italy), Sep. 6-8 2010.

[4] D. Vaes, K. Engelen, J. Anthonis, J. Swevers, and P. Sas, "Multivariable feedback design to improve tracking performance on tractor vibration test rig," *Mechanical Systems and Signal Processing*, vol. 21, pp. 1051–1075, 2007.

[5] L. Zuo and J. Slotine, "Robust vibration isolation via frequency-shaped sliding control and modal decomposition," *Journal of Sound and Vibration*, vol. 285, no. 4-5, pp. 1123 – 1149, 2005.

[6] D. Karnopp, "Active and semi-active vibration isolation," *Journal of Mechanical Design*, vol. 117, pp. 177–185, 1995.

[7] K. WATANABE, S. HARA, Y. KANEMITSU, T. HAGA, and K. YANO, "Combination of h_∞ and pi control for an electromagnetically levitated vibration isolation system," in *Proc. 35th Conference on Decision and Control*, (Kobe, Japan), Dec. 1996.

[8] C. Ding, A. Damen, and P. van den Bosch, "Robust vibration isolation by frequency-shaped sliding surface control with geophone dynamics," in *Proc. of IECON 2010*, (Glendale, Phoenix, AZ. USA.), Nov. 2010.

[9] K. Young, V. Utkin, and U. Ozguner, "A control engineer's guide to sliding mode control," *IEEE Transactions on Control Systems Technology*, vol. 7, no. 3, pp. 328–342, 1999.

[10] A. Barzilai, T. VanZandt, and T. Kenny, "Technique for measurement of the noise of a sensor in the presence of large background signals," *Review of Scientific Instruments*, vol. 69, no. 7, 1998.

[11] M. Heertjes, K. d. Graaff, and J. v. d. Toorn, "Active vibration isolation of metrology frames; a modal decoupled control design," *ASME Journal of Vibration and Acoustics*, vol. 127, no. 3, pp. 223–233, 2005.